Instability In Magnetic Mirror Configuration

Hunt Feng

May 9, 2023

Contents

Chapter 1

Introduction

1.1 Flow in Magnetic Mirror Configuration

Plasma flow in magnetic mirror configurations have been studied extensively in plasma physics due to its frequent precense in many areas such as the accretion flow[4, 1] , and magnetic nozzle[7]. However, the stability of these configurations remains a debatable subject.

Despite these efforts, the stability of magnetic mirror configurations remains a topic of active research. New diagnostic techniques and advanced numerical simulations are being developed to improve our understanding of the underlying physics and guide the design of more stable magnetic nozzle.

1.1.1 Magnetic Nozzle

Magnetic nozzle is a convergent-divergent magnetic field that guides, expands and accelerates a plasma jet into vacuum for the purpose of space propulsion. [2, 3, 9] The configuration is of the magnetic field in the magnetic nozzle plays a similar role to the walls of a Laval nozzle, see Fig. 1.1. The plasma flow starts from subsonic at one end can be accelerated to supersonic at the exit.

1.1.2 Accretion Flow

Accretion flow is similar to that in magnetic nozzle. The plasma flow is at rest at infinity and accelerated towards the steller object due to gravity. It is natural to compare the study of its instabilities to that of magnetic nozzle. However, the results are still debatable. [5, 1, 8]

1.2 Goals of this Thesis

The goals of this thesis is to first study the spectral method for solving the instability problem. When using the spectral method, it is necessary to under-

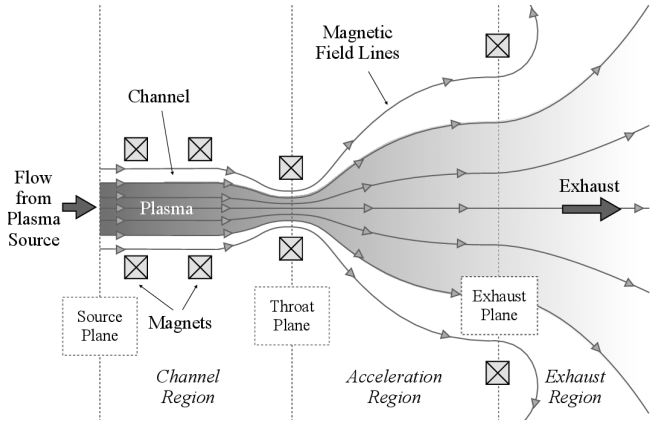

Figure 1.1: Example of a magnetic nozzle configuration. In our models, we define the magnetic nozzle as the region downstream from the throat plane, which can be further divided into an acceleration region and exhaust region. The channel connects the plasma source (not shown) with the magnetic nozzle. [6]

stand different discretizations of the operators, such as finite difference, finite element and spectral element method.

Once the spectral method is introduced, we can use it to study the instability of plasma in magnetic nozzle. We can use different discretization techniques, and compare the results from different methods.

Finally, we need to take care of the filtering of the spectral pollution.

Chapter 2

Governing Equations

2.1 Governing Equations for Flow in Magnetic Nozzle

In this section, we will derive the governing equations of the flow in magnetic nozzle, starting from the fluid description for plasma.

In magnetic nozzle, the magnetic field is along the nozzle, which we denote as z-axis. Due to Lorentz force, the charged particles gyrates about the magnetic field lines. Because the magnetic moment is invariant in such situation (**reference**). The fluid velocity of particles can be written as $\mathbf{v} = v\mathbf{B}/B$, meaning that the particles move along the magnetic field lines. Therefore the conservation of density

$$\frac{\partial n}{\partial t} + \boldsymbol{\nabla} \cdot (n\mathbf{v}) = 0 \Rightarrow \frac{\partial n}{\partial t} + B\frac{\partial}{\partial z}\Big(\frac{nv}{B}\Big) = 0$$

In the derivation, $\boldsymbol{\nabla} \cdot \mathbf{B} = 0$ is used.

To derive the second governing equation, we start from the conservation of momentum,

$$\frac{\partial v}{\partial t} + v\frac{\partial v}{\partial z} = -\frac{1}{\rho}\boldsymbol{\nabla} p$$

Let $\boldsymbol{\nabla} p = k_B T\ \partial n/\partial z$, we have

$$\frac{\partial v}{\partial t} + v\frac{\partial v}{\partial z} = -c_s^2\frac{1}{n}\frac{\partial n}{\partial z}$$

where $c_s^2 = k_B T/m$ is the square of sound speed.

Therefore the dynamics of the flow in magnetic nozzle can be characterized by the conservation of density and momentum,

$$\frac{\partial n}{\partial t} + B\frac{\partial}{\partial z}\Big(\frac{nv}{B}\Big) = 0$$
$$\frac{\partial v}{\partial t} + v\frac{\partial v}{\partial z} = -c_s^2\frac{1}{n}\frac{\partial n}{\partial z}$$

The discussion of magnetic field is in next subsection.

2.1.1 Magnetic Field in Magnetic Nozzle

In 1D problem, the magnetic field is given by

$$B(z) = B_0 \left[1 + R \exp\left(-\left(\frac{x}{\delta}\right)^2\right)\right]$$

where $1 + R$ is the magnetic mirror ratio, and δ determines the spread of the magnetic field. It is shown in Fig.(2.1).

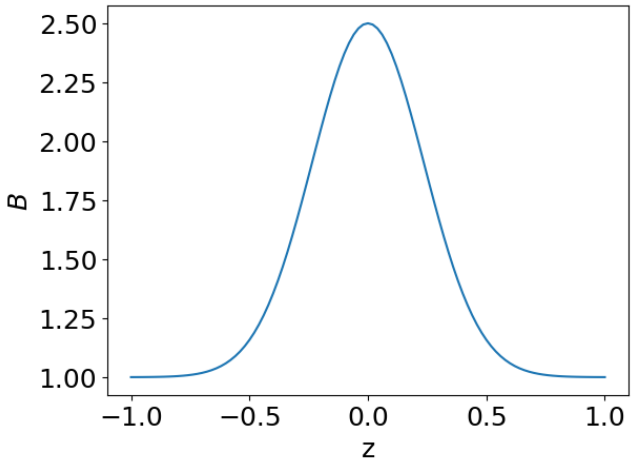

Figure 2.1: This is the magnetic field in nozzle with mirror ratio $1 + R = B_{max}/B_{min} = 2.5$, and the spread of magnetic field, $\delta = 0.1/0.3 = 0.\bar{3}$.

2.1.2 Velocity Profile at Equilibrium

Let n_0 and v_0 be the density and velocity at equilibrium (stationary solution), we know that $\partial n_0/\partial t = 0$ and $\partial v_0/\partial t = 0$, therefore n_0 and v_0 satisfy the so-called equilibrium condition,

$$\frac{\partial}{\partial z}\left(\frac{n_0 v_0}{B}\right) = 0$$
$$v_0 \frac{\partial v_0}{\partial z} = -c_s^2 \frac{1}{n_0}\frac{\partial n_0}{\partial z}$$

Let $M(z) = v_0(z)/c_s$ be the mach number (nondimensionalized velocity). The equations of motion become

$$B\frac{\partial}{\partial z}\left(\frac{n_0 M}{B}\right) = 0$$
$$M\frac{\partial M}{\partial z} = -\frac{1}{n_0}\frac{\partial n_0}{\partial z}$$

Substitute $\frac{1}{n_0}\,\partial n_0/\partial z$ using first equation, the conservation of momentum becomes

$$(M^2-1)\frac{\partial M}{\partial z} = -\frac{M}{B}\frac{\partial B}{\partial z}$$

Notice that there is a singularity at $M=1$, the sonic speed.

This is a separable equation, integrate it and use the conditions at midpoint $B(0)=B_m, M(0)=M_m$ we get

$$M^2 e^{-M^2} = \frac{B^2}{B_m^2} M_m^2 e^{-M_m^2}$$

We can now express M using the Lambert W function,

$$M(z) = \left[-W_k\left(-\frac{B(z)^2}{B_m^2} M_m^2 e^{-M_m^2}\right)\right]^{1/2}$$

where the subscript k of W stands for branch of Lambert W function. When $k=0$, it is the subsonic branch; When $k=-1$, it is the supersonic branch. Below shows a few cases of the solution.

- $M_m < 1, k=0$, subsonic velocity profile.
- $M_m = 1$, $k=0$ for $x<0$ and $k=-1$ for $x>0$, accelerating profile
- $M_m = 1$, $k=-1$ for $x<0$ and $k=0$ for $x>0$, decelerating profile
- $M_m > 1, k=-1$, supersonic velocity profile

Fig.(2.2) shows some cases of the solution.

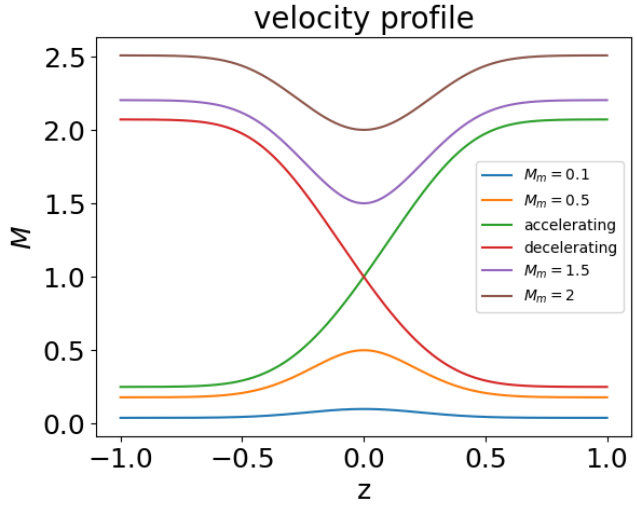

Figure 2.2: The velocity profile in the magnetic nozzle is completely determined by M_m, the velocity at the midpoint, $z=0$. For the transonic velocity profiles, M_m alone is not enough to determine the profile, we need to specify the branch of Lambert W function to determine whether it is accelerating or decelerating.

2.2 Linearized Equations

For convenience, we nondimensionalize the governing equations by normalizing the velocity to c_s, $v \mapsto v/c_s$, z to system length L, $z \mapsto z/L$ and time $t \mapsto c_s t/L$. The governing equations become

$$\frac{\partial n}{\partial t} + n\frac{\partial v}{\partial z} + v\frac{\partial n}{\partial z} - nv\frac{\partial_z B}{B} = 0 \tag{2.1}$$

$$n\frac{\partial v}{\partial t} + nv\frac{\partial v}{\partial z} = -\frac{\partial n}{\partial z} \tag{2.2}$$

and the nondimensionalized equilibrium condition is

$$\frac{\partial}{\partial z}\Big(\frac{n_0 v_0}{B}\Big) = 0 \tag{2.3}$$

$$v_0\frac{\partial v_0}{\partial z} = -\frac{1}{n_0}\frac{\partial n_0}{\partial z} \tag{2.4}$$

Now we are going to derive an important intermediate result, the linearized governing equations.

Proposition 1. *Let $n = n_0(z) + \tilde{n}(z,t)$ and $v = v_0(z) + \tilde{v}(z,t)$, where $\tilde{n}$ and $\tilde{v}$ are small perturbed quantities. The linearized governing equations are*

$$\frac{1}{n_0}\frac{\partial \tilde{n}}{\partial t} + \frac{\partial \tilde{v}}{\partial z} + v_0\tilde{Y} + \tilde{v}\frac{\partial_z n_0}{n_0} - \tilde{v}\frac{\partial_z B}{B} = 0 \tag{2.5}$$

$$\frac{\partial \tilde{v}}{\partial t} + \frac{\partial(v_0\tilde{v})}{\partial z} = -\tilde{Y} \tag{2.6}$$

where

$$\tilde{Y} \equiv \frac{1}{n_0}\frac{\partial \tilde{n}}{\partial z} - \frac{\partial_z n_0}{n_0^2}\tilde{n} = \frac{\partial}{\partial z}\left(\frac{\tilde{n}}{n_0}\right)$$

2.3 Formulation of the Problem

In order to investigate the instability of magnetic nozzle, we need formulate it as an eigenvalue problem. To do that, we assume the perturbed density and velocity are oscillatory, i.e. $\tilde{n}, \tilde{v} \sim \exp(-i\omega t)$, where ω is the oscillation frequency of the perturbed quantities. This frequency can be a complex number. If $\omega = \omega_r + i\omega_i$, then the perturbed quantities becomes $\tilde{n} \sim \exp(\omega_i t)\exp(i\omega_r t)$, which means it grows exponentially with time.

Proposition 2. *Let $\tilde{n} \sim \exp(-i\omega t)$ and $\tilde{v} \sim \exp(-i\omega t)$, then we have the polynomial eigenvalue problem*

$$\omega^2\tilde{v} + 2i\omega\left(v_0\frac{\partial}{\partial z} + \frac{\partial v_0}{\partial z}\right)\tilde{v} + \left[(1-v_0^2)\frac{\partial^2}{\partial z^2} - \left(3v_0 + \frac{1}{v_0}\right)\frac{\partial v_0}{\partial z}\frac{\partial}{\partial z} - \left(1 - \frac{1}{v_0^2}\right)\left(\frac{\partial v_0}{\partial z}\right)^2 - \left(v_0 + \frac{1}{v_0}\right)\frac{\partial^2 v_0}{\partial z^2}\right]\tilde{v} = 0 \tag{2.7}$$

Next step we can decouple this equation so that it becomes an eigenvalue problem.

$$\begin{bmatrix} 0 & 1 \\ \hat{M} & \hat{N} \end{bmatrix} \begin{bmatrix} \tilde{v} \\ \omega\tilde{v} \end{bmatrix} = \omega \begin{bmatrix} \tilde{v} \\ \omega\tilde{v} \end{bmatrix} \tag{2.8}$$

where O is zero matrix, I is identity matrix, and

$$\hat{M} = -\left[(1 - v_0^2)\frac{\partial^2}{\partial z^2} - \left(3v_0 + \frac{1}{v_0}\right)\frac{\partial v_0}{\partial z}\frac{\partial}{\partial z} - \left(1 - \frac{1}{v_0^2}\right)\left(\frac{\partial v_0}{\partial z}\right)^2 - \left(v_0 + \frac{1}{v_0}\right)\frac{\partial^2 v_0}{\partial z^2} \right]$$

$$\hat{N} = -2i\left(v_0\frac{\partial}{\partial z} + \frac{\partial v_0}{\partial z}\right)$$

This becomes an algebraic eigenvalue problem if we discretize the operators and the function $\tilde{v}$.

Chapter 3

Numerical Experiments

In this chapter, we will solve the eigenvalue problem, Eq.(2.8), with different discretizations. There will be three major categories of methods used. Finite difference (FD) method, finite element (FE) method and spectral element method (SE).

The finite difference method will be used together with equally spaced nodes. The finite element method will use B-spline as basis functions. Finally, the spectral element method uses sine functions as the spectral elements.

For Dirichlet boundary, The parameters of different discretizations are listed below

Table 3.1: With Dirichlet boundary condition, all methods have good accuracy, so using 101 nodes in the region $[0, 1]$ is enough. For FE and SE methods, they are using 50 basis functions.

	FD	FE_BSPLINE	SE_SINE
N	101	101	101
NUM_BASIS		51	50

For left-fixed and right-open (fixed-open) boundary condition, the parameters are

Table 3.2: With fixed-open boundary condition, it requires higher resolution in order to get accurate results. Therefore all methods use 501 nodes in the region $[0, 1]$, and FE method uses 101 basis functions.

	FD	FE_BSPLINE
N	501	501
NUM_BASIS		101

3.1 Constant Velocity Case

3.1.1 Dirichlet Boundary

Because the existence of exact solution to problems Eq.(**??**). The case with constant velocity profile is used as a sanity check. It allows us to verify the correctness of each method's implementation. This also serves as a reference to the accuracy spectral methods can achieve.

From Fig.(**??**), we see that the order of growth rates obtained by different methods is about 10^{-14} for both subsonic and supersonic cases. We will use these numbers as a reference to the accuracy of our numerical methods. If a method produces growth rates with order close to 10^{-14}, we consider the growth rates to be 0.

Table 3.3: Relative error of each eigenvalue.

$v_0 = 0.5$	1	2	3	4	5
FD	2.827e-05	1.130e-04	2.541e-04	4.512e-04	7.040e-04
FE	0.005	0.005	0.006	0.008	0.010
SE	2.896e-05	1.157e-04	2.603e-04	4.626e-04	7.217e-04

$v_0 = 1.5$	1	2	3	4	5
FD	0.001	0.005	0.010	0.019	0.030
FE	0.006	0.010	0.019	0.029	0.043
SE	0.001	0.005	0.011	0.019	0.030

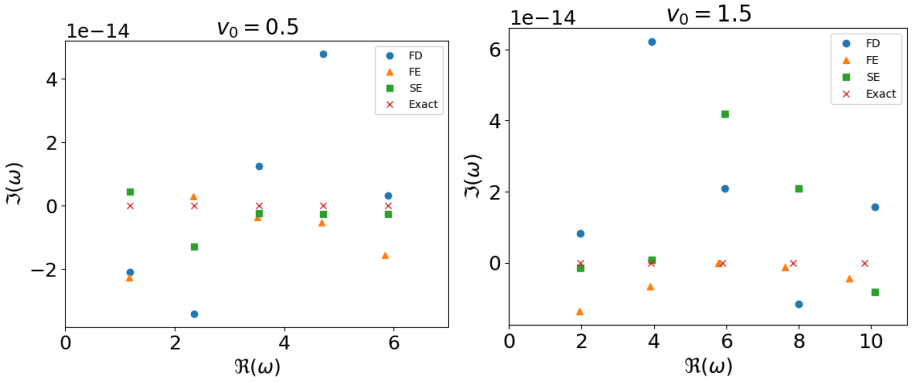

(a) All modes are stable.

(b) Filtered modes are stable.

Figure 3.1: Showing the first 5 eigenvalues of each method in each case. All methods are close to the exact eigenvalues.

3.1.2 Fixed-Open Boundary

Table 3.4: Relative error of each eigenvalue. Notice that the ground mode for subsonic case is non-zero.

$v_0 = 0.5$	0	1	2	3	4
FD	1.209e-05	3.458e-05	5.775e-05	8.153e-05	1.061e-04
FE	8.090e-05	2.007e-04	2.981e-04	6.596e-04	1.821e-03
$v_0 = 1.5$	1	2	3	4	5
FD	9.163e-05	2.435e-04	4.833e-04	8.160e-04	1.243e-03
FE	4.431e-04	7.924e-04	1.516e-03	3.103e-03	8.001e-03

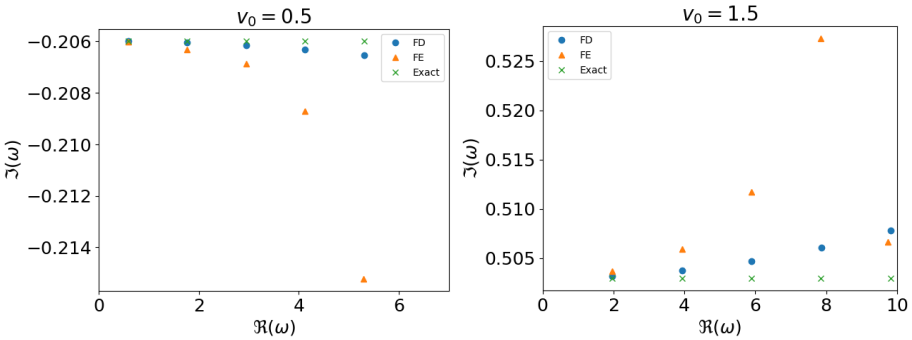

(a) All modes are stable.

(b) All modes are unstable.

Figure 3.2: Showing the first 5 eigenvalues of each method. Finite-difference method has much better accuracy than finite-element method.

3.2 Subsonic Case

3.2.1 Dirichlet Boundary

When setting the mid-point velocity to be $M_m = 0.5$, we have the subsonic velocity profile. This velocity profile is the orange line shown in Fig.**??**. With Dirichlet boundary condition, $\tilde{v}(\pm 1) = 0$. The flow in magnetic nozzle is stable. Fig.3.3 shows the first few eigenvalues obtained by different discretizations.

The order of growth rates obtained by different methods is 10^{-13}, we can consider it to be stable.

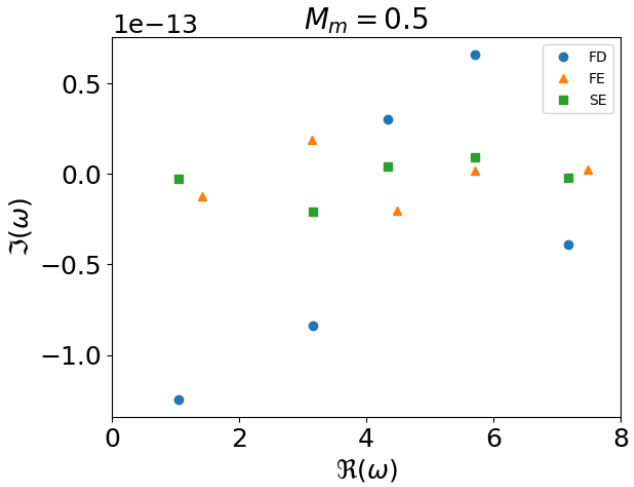

Figure 3.3: Showing the first 5 modes. It suggests that the flow in magnetic nozzle with subsonic velocity profile and Dirichlet boundary condition is stable.

3.2.2 Fixed-Open Boundary

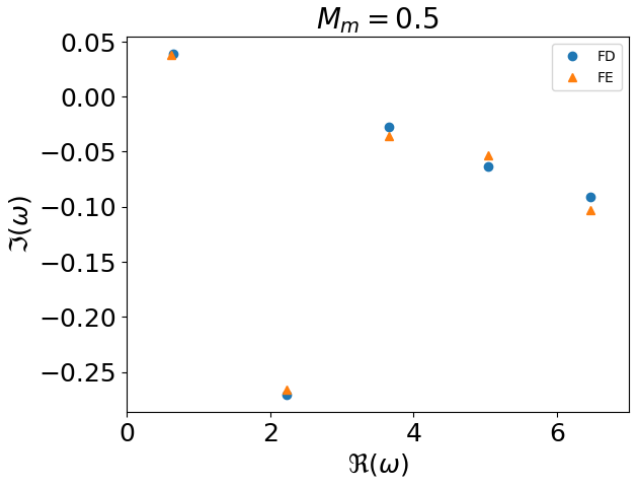

Figure 3.4: Showing the first 5 modes. The ground mode is unstable, other modes are stable.

3.3 Supersonic Case

3.3.1 Dirichlet Boundary

When the velocity profile is supersonic, shown as purple line in Fig.**??**, spurious modes appeared as predicted in Chap.**??**. Using the convergence test, we successfully eliminates all unstable modes. Fig.(3.5) shows the first few filtered eigenvalues. As we can see the flow is stable.

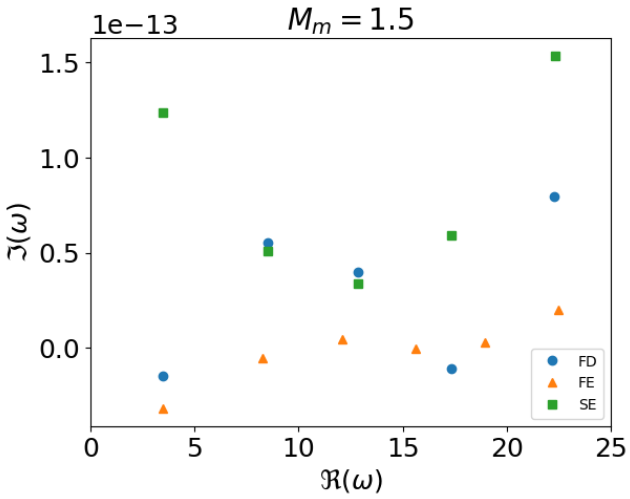

Figure 3.5: First few filtered eigenvalues are shown. The spurious modes are filtered by convergence test.

3.3.2 Fixed-Open Boundary

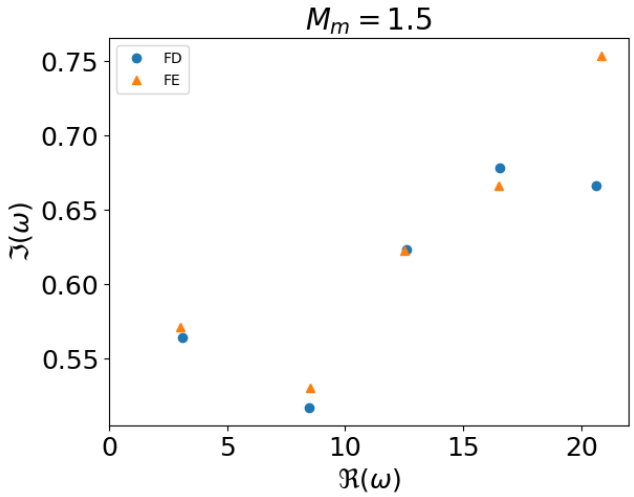

Figure 3.6: All modes are unstable.

3.4 Accelerating Case

3.4.1 Dirichlet Boundary

In this case, the flow starts from subsonic speed and accelerates to supersonic case, the velocity is exactly at sonic point $M_m = 1$ at the center of the magnetic nozzle as shown in Fig.(**??**) With Dirichlet boundary condition, spectral method with different discretizations gave negative eigenvalues. This indicates that the perturbation $\tilde{v}$ is damped oscillation, its amplitude will be decrease to zero exponentially in time, $\tilde{v} \sim \exp(\mathrm{Im}(\omega)t)$. Hence, the flow in magnetic nozzle is stable.

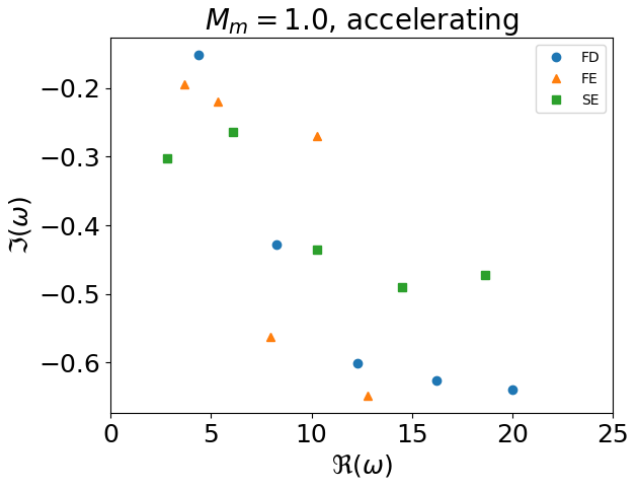

Figure 3.7: The filtered eigenvalues are negative. This indicates that the perturbation $\tilde{v}$ is a damped oscillation, their amplitude will decrease to zero as time elapse.

3.4.2 Fixed-Open Boundary

These numerical methods do not work well in this case. It is hard to conclude whether or not the flows are stable.

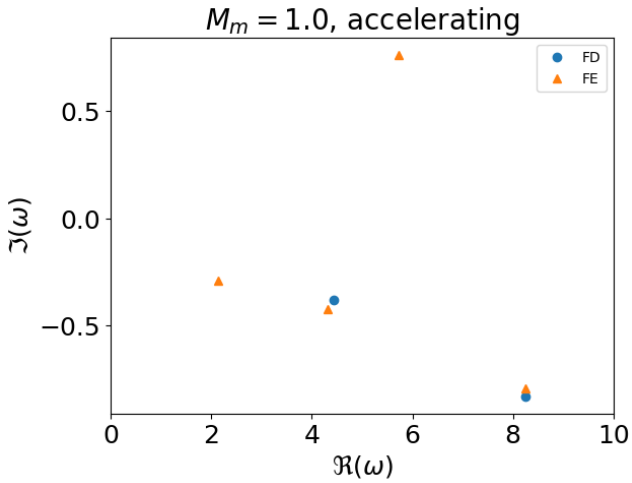

Figure 3.8: Hard to tell.

3.5 Decelerating Case

3.5.1 Dirichlet Boundary

As predicted by Proposition.??, the growth rates must be positive since they are complex conjugates of the eigenvalues in accelerating case.

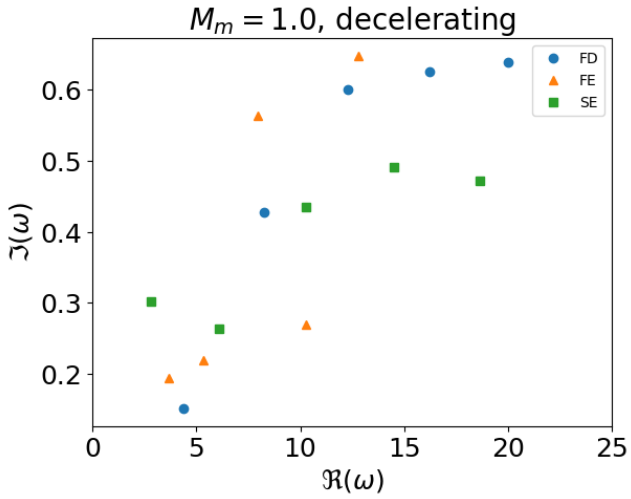

Figure 3.9: The flow with decelerating velocity profile and Dirichlet boundaries is unstable. The grow rates are opposite to that in accelerating case.

3.5.2 Fixed-Open Boundary

These numerical methods do not work well in this case. It is hard to conclude whether or not the flows are stable.

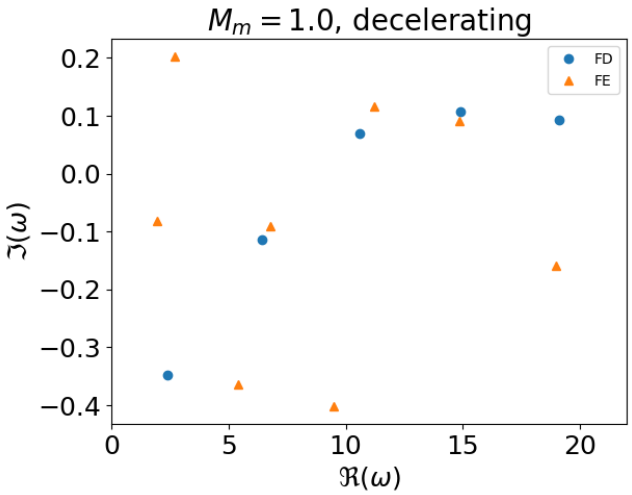

Figure 3.10: Hard to tell.

Chapter 4

Future Work

This research is still in its beginning. To improve the credibility of the results, different numerical calculation methods will be employed.

- Investigate the solution of the problem near the singular point.
- Try to match the eigenfunctions to a non-zero left boundary and investigate the corresponding instabilities.
- Setup a analytically solvable problem with similar configuration. Compare the analytical results to the the experimental computations to better understand the physics.

Bibliography

[1] Toshiki Aikawa. The stability of spherically symmetric accretion flows. *Astrophys Space Sci*, 66(2):277–285, December 1979.

[2] S. A. Andersen. Continuous Supersonic Plasma Wind Tunnel. *Phys. Fluids*, 12(3):557, 1969.

[3] R. W. Boswell, O. Sutherland, C. Charles, J. P. Squire, F. R. Chang Díaz, T. W. Glover, V. T. Jacobson, D. G. Chavers, R. D. Bengtson, E. A. Bering, R. H. Goulding, and M. Light. Experimental evidence of parametric decay processes in the variable specific impulse magnetoplasma rocket (VASIMR) helicon plasma source. *Physics of Plasmas*, 11(11):5125–5129, November 2004.

[4] Klaus Jockers. On the stability of the solar wind. *Sol Phys*, 3(4):603–610, April 1968.

[5] Eric Keto. Stability and solution of the time-dependent Bondi–Parker flow. *Monthly Notices of the Royal Astronomical Society*, 493(2):2834–2840, April 2020.

[6] Justin M Little. Performance scaling of magnetic nozzles for electric propulsion, 2015. ISBN: 9781321565317.

[7] A. I. Smolyakov, A. Sabo, P. Yushmanov, and S. Putvinskii. On quasineutral plasma flow in the magnetic nozzle. *Physics of Plasmas*, 28(6):060701, June 2021.

[8] R. F. Stellingwerf and J. Buff. Stability of astrophysical gas flow. I - Isothermal accretion. *ApJ*, 221:661, April 1978.

[9] Craig H. Williams. Fusion Propulsion Through a Magnetic Nozzle and Open Divertor. In *AIP Conference Proceedings*, volume 654, pages 510–515, Albuquerque, New Mexico (USA), 2003. AIP. ISSN: 0094243X.